International Journal of Applied Engineering Research ISSN 0973-4562 Volume 12, Number 24 (2017) pp. 14702-14709
© Research India Publications. http://www.ripublication.com

Development and Characterization of the PMMA/Clay Nanocomposite

Nurul Shafrah Shaharil[1]

[1]*Universiti Kuala Lumpur Malaysia France Institute,*
Section 14, Jalan Teras Jernang, 43650 Bandar Baru Bangi, Selangor, Malaysia.

Abstract

Usually used as the main material in optical components such as lenses, objectives and plastic optical fiber, Polymethylmethacrylate (PMMA) or Perspex is an excellent optical polymeric material. In the article, the development method of the nanocomposite clay/PMMA and the effects of different nanoclay concentration on properties of PMMA/nanoclay composite were investigated. This study was also intended to determine optimal content of nanoclay within PMMA matrix which produced optimal enhancement. Various contents of nanoclay (from 0 to 7 phr) are blended with PMMA using several techniques, of which melt intercalation appeared to deliver the best result. The samples were put under tensile, impact, hardness and flexural tests to investigate their mechanical properties. TEM imaging and XRD analysis showed that the intercalation has occurred for sample (1,3 and 5 phr). As for their tensile properties, the nanocomposite exhibited improvements at certain level of nanoclay concentration.

Keywords: Intercalation, montmorillonite nanoclay, nanocomposite, polymer.

INTRODUCTION

Growing interest in the development of polymer-nanocomposite material during these few decades has led to a new technological approach, which on the other hand, revealed another dimension of material science. The development of polymer-nanocomposites resulted in non-exhaustive possibilities of novel physical properties and functionalities, beyond those of conventional composite. A polymer-nanocomposite consists of embedded inorganic particles of at least one dimension in nanometer scale in the matrix phase of an organic polymer, whether in form of fibers, sheets or particles [1]. The nanoparticles enhance certain mechanical properties of the polymer-nanocomposite such as stiffness, heat deflection temperature, dimensional stability, flame retardancy and reduced gas permeability by acting as reinforcing agents [1][2].

The prominent usage of nanoclay as a filler in the polymer matrix phase has captured great attention from both the research and industrial world, mainly because it is cost-competitive, ecologic and easily accessible. On the other hand, further investigations indicate that the mechanical properties of pristine polymers could be substantially enhanced by loading a very low amount of nanoclay [3]. The high-aspect ratio and high-surface area of the nanoclay contribute to great reinforcement effects on the polymer matrix.

Naturally occurring in abundance, nanoclays are in fact nanoparticles built of layered mineral silicates, of which montmorillonite is the most common representative. However, natural layered silicates are hydrophilic, thus incompatible with most organic molecules. They disperse in hydrophobic polymers with great difficulty and form agglomerates. To render layered silicates compatible with polymer matrix, they must first be organically modified to become hydrophobic [4]. This modification permits the miscibility of layered silicates with polymer matrix by expanding its gallery spacing, thus letting in the molecules of the polymer within the galleries, hence the dispersion [5]. Two types of composite micro-structure are achievable depending on the nature and properties of clay and polymer as shown (Figure 1) [6]:

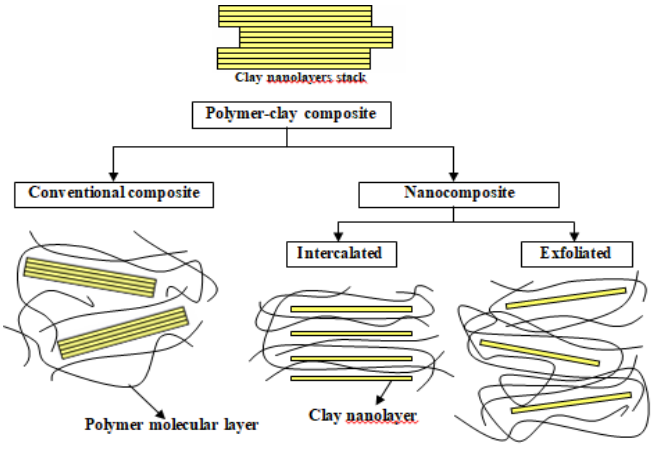

Figure 1: Structure of polymer-clay composite

Conventional composite

An organic polymer interacting with unmodified clay produces conventional composite. It contains aggregated clay particles, leading to phase separated structure. The stacks of

clay nanolayers retained as a whole within polymer matrix, thus preventing the intercalation of polymer molecules into the clay micro-structure. The properties of the conventional composite do not differ much from traditional micro-composite.

Nanocomposite

On the other hand, polymer-clay nanocomposite can be structurally intercalated or, better, exfoliated. Intercalated structure occurs when one or a few molecular layers of polymer are inserted within the gallery, thus weakening the electrostatic forces between the layers, and cause to the increasing of interlayer spacing. However, the remaining electrostatic forces are strong enough to keep the array of clay nanolayer well-ordered.

As for exfoliated nanocomposite, the nanolayers are individually dispersed in the polymer matrix and no longer attached by electrostatic forces between them. They lost their original arrangement of array due to disruption of the layers caused by gallery expansion (interlayer spacing more than 80-100 Å [7]). Therefore, each and every nanolayer is fully-contributed to interfacial interactions with the matrix, resulting in greater phase homogeneity. The exfoliated nanocomposite exhibits most significant properties improvement compared to the rest.

In general, it is possible to prepare polymer-clay nanocomposites via solution intercalation, in-situ intercalative polymerization, in-situ template synthesis or melt intercalation or extrusion. However, during the development of PMMA/clay nanocomposite session, several attempts via solution intercalation were to no avail as samples produced were not homogeneous even to naked eyes. Previous study revealed that a thorough dispersion of the nanoclay within the matrix of plastic material was technically difficult to achieve [8].

Solution Intercalation

This technique involved dissolving PMMA pellets with organic solvent such as acetone for several hours, followed by the addition of the modified nanoclay of 1phr, Dioctyl Phtalate (DOP) 20% and methanol 2%. DOP played the role as a softening agent in order to aid the dissolving process of PMMA pellets, while methanol as deformer. The solution was then sonicated for another hour or two to eliminate the air bubbles until it got clear and transparent. The sample is obtained by solvent removal through precipitation and vaporization.

Theoretically, the nanoclay would be swollen in acetone solvent. As the PMMA pellets dissolve in the solvent, its chains would get absorbed onto the delaminated sheets of the nanoclay. This polymer chains would diffuse between the interlayer spacings of nanoclay during the solvent evaporation, filling in the empty spacing between the layers left by the solvent molecules [9].

However, the sample produced afterwards exhibits two distinct phases. The majority of the sample was white opaque whereas a small area near the border was transparent. The separate phases suggest the inhomogeneous nanoclay blend-in within the PMMA matrix. The problem might originate from the solvent itself as it is difficult to make sure that the solvent is removed thoroughly during the evaporation, which will intervene in the dispersion of nanoclay. The outcome sample was also found brittle and unsuitable for mechanical testing. Further reading suggests that resin viscosity and duration of sonication are the parameters that might lead to the brittling of resultant nanocomposite, as overly mixture sonication leads to early curing of the resin [10].

Melt intercalation method, on the other hand, does not require a solvent, as nanoclay is mixed within polymer matrix in the molten state, followed by extrusion and injection moulding.

EXPERIMENTAL (MELT INTERCALATION METHOD)

Materials

Polymethyl methacrylate (PMMA) acrylic beads BS 150N of Altuglas® BS grades of diameter 50 μm and bulk density of 0.6 g/cm^3 from Arkema Group. The density of pure PMMA (0 phr) is measured at 1.1924 g/cm^3.

Nanoclay Montmorillonite, labelled respectivey as **N5** in the following paragraphs, exchanged with dimethyl dihydrogenated tallow quaternary ammonium (Cloisite 20A) was purchased from Southern Clay Products Inc. USA.

Ultra-Plast TP10 compatibilizer of specific gravity 0.95 g/cm^3 and dropping point of 100°C from laboratory.

Sample preparation

Prior to blending, crushed PMMA acrylic beads and nanoclay were subjected to preheating in vacuum oven at 80°C for 24h in order to remove excessive moisture. Polymer nanocomposite PMMA/Nanoclay blends were prepared at various nanoclay filler content (0, 1, 3, 5 and 7 phr). The melt intercalation aided by processing additive Ultra-Plast TP10 was performed by a Brabender twin screw extruder (Brabender GmbH, Duisburg, Germany). Materials were loaded into the extruder while being heated to molten state. The obtained molten compound was forced through a die and shaped into long cylindrical rod. The rod solidified as it passed through water at room temperature and eventually pelletized. The pellets passed through injection mould machine to produce several forms of standard-sized specimen for mechanical testing.

Characterization

The developed nanocomposite sample were characterised by a variety of microscopic and macroscopic techniques. The dispersion of the nanoclay was investigated by XRD and TEM. XRD analysis were recorded on a Shimadzu XRD 600 X-Ray diffractometer, the Xray beam was nickel filtered CuKα (λ=1.542Å) and data obtained were from 2θ of 1° to 6°.

The electron transmission images were obtained using LEO 912AB energy filter transmission electron microscope with an acceleration voltage of 120 keV. For sampling purpose, thin sections of about 90 nm were prepared using the diamond blade of Reichert Jung Ultracut E microtome, cooled at -120°C and equipped with cryo-sectioning unit.

The tensile test was measured by means of an Instron model 4301 testing machine (cell load 1kN) according to ASTM D638, using dumbbell-shaped specimens which were extended at a crosshead speed of 10 mm/min. The machine measures the force required to pull apart the specimen and also the amount of stress it undergoes before breaking up.

The relative impact resistance test was carried out by Izod-Impact Ceast testing machine according to ASTM D256. The tester was loaded with 4 Joules-load and hit the specimens of dimensions 6x1.2x0.4 cm at the bottom. The machine measures energy lost per unit thickness (J/m) under controlled laboratory conditions.

The hardness test was done by a Zwick/Roell durometer hardness according to ASTM D2240 using a Shore D Hardness probe. The durometer measures the penetration of an indenter into 5 test points marked on 7x7x0.33 cm test specimen as a force of 5 Newtons is loaded.

The flexural test (ASTM D790) was performed using an Instron model 4301, measuring the force required to bend a beam of specimen under three point loading conditions. The specimen of size 12.7x1.27x0.33 cm lies on a support span of 48 mm while a load of 1kNewton is applied to the centre, producing three-point bending at a speed rate of 1.14 mm/min. Once the specimen broke, the machine stopped and gave out the value of flexural modulus elasticity in bending, the maximum force applied on the specimen and the maximum amount of stress undergone by the specimen just before it broke apart.

The specific gravity test measuring the density of solid PMMA/N5 compound, was performed by an electronic densimeter Mirage MD-200S. A piece of the sample is weighed comparatively under atmosphere pressure and also under water according to the principle law of Archimedes. The measurements give out its density value in g/cm^3.

The haze transmission and total transmittance tests were prepared according to ASTM 1003 by BYK-Gardner Haze-Dual Plus hazemeter. The specimen surface is illuminated perpendicularly by placing it between the fraction port of the integrating sphere and the source of illumination, whereas the transmitted light is measured by the photodiode, placed behind the light trap. The spectral sensitivity conforms to the CIE standard spectral value under standard lamp D65, which is a noon daylight illuminant (6504° Kelvin).

The gloss test (ASTM D523) was performed by BYK-Gardner Micro-tri-gloss tester. The ability of the surface of the specimen to reflect an incident beam of light of incident angles of 20°, 60° and 85° into specular direction was registered and reported in Gloss Unit (G.U). The results were calibrated to the amount of reflected light from a standard black glass with defined refractive index of 100 G.U.

The abrasion resistance test according to ASTM D1044 and ASTM D4060 was done by Taber Rotary Platform Abraser model 5155. The specimen was a disk of 10.5 mm in diameter, 3 mm thick and had a circular hole of 0.5 cm diameter to fix into the holder of the tester. A load of 1000 grams was placed on top of the abrader wheels, coated with sandpaper strips and took 10 revolutions of spinning. During this test, the ability of the nanocomposite to withstand mechanical actions such as rubbing, scraping or erosion was tested in order to quantify the change in % haze and weight loss in mg/10 cycles.

All measures reported here represent an average of the results from tests run twice on five specimens.

RESULTS AND DISCUSSION

XRD Analysis

XRD analysis evaluates the degree of interfacial interaction of the nanoclay layers within the polymer matrix, whether the microstructure intercalates, or exfoliates. When the X-ray beam is incident on the microstructure, it will be diffracted by atomic planes of nanoclay's regular layered structure, depicting diffractogram of characteristic peaks (Figure 2).

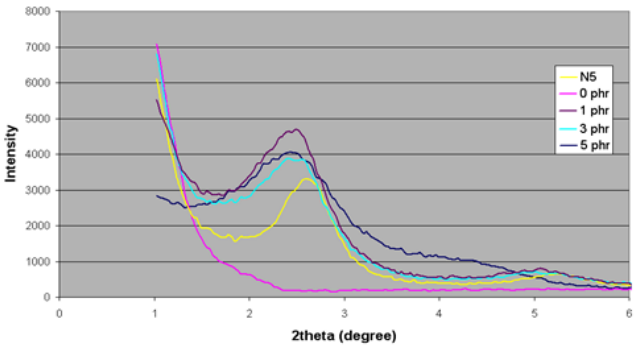

Figure 2: XRD Diffractogramme of various nanoclay content in PMMA matrix

The above diffractogram illustrates the diffraction peaks of various content of nanoclay in the PMMA polymer matrix. At 0 phr, no peak was detected as the sample did not contain nanoclay. The absence of nanoclay's structured layer results

in the indiffraction of the X-ray beam, hence no diffraction peak.

According to Bragg's Law, the lattice spacing of nanoclay layers is modified by polymer intercalation when there are changes in the peak position, the peak broadness and also the peak intensity. A control was established, where organically modified nanoclay, labelled here as N5, was analysed, and its peak position is registered at 2θ =2.71°. As the content of nanoclay increased within polymer matrix, the diffraction peak shifted slightly to a lower diffraction angle, 2θ =2.41°, suggesting the increasing of the interlayer distance of nanoclay . The broadening of the diffraction peak can be seen, as well as the increasing intensity in function of nanoclay content, indicating that polymer molecules have intercalated within the galleries of silicate nanolayer.

Using Bragg formula: $\lambda = 2d \sin\theta$, where λ is the X-ray wavelength (1.542 Å) and θ can be obtained from the diffractogramme, we can determine the value of basal spacing (or d-spacing) of nanolayer. Organically modified nanoclay possessed a basal spacing of 3.20nm, while increasing nanoclay content from 1 to 5 phr led to a basal spacing of 3.7 nm. The variation of basal spacing is probably due to the amount of polymer penetrating between the silicate nanolayer.

It is also interesting to point out that increasing nanoclay from 1 to 5 phr within PMMA polymer matrix didn't result in the shifting of their diffraction peaks distinctly to much lower angle. The d-spacing between the sheets of silicate nanolayer seems to be unaffected by the amount of nanoclay beyond 1 phr. Increasing nanoclay content might as well resulted in agglomeration of nanoclay within polymer matrix as their interlayer distance remains constant.

3.2. TEM Imaging

In addition to XRD analysis, TEM images provide qualitative observation of nanocomposite's microstructure by revealing the spatial dispersion of nanoclay layers within the polymer matrix. The following micrographs Figure the morphology of the nanocomposite with 5,3 and 1 phr nanoclay contents at 40kX magnification (Figure 3, 4 and 5).

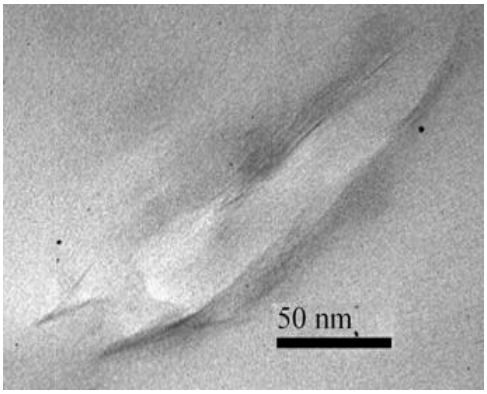

Figure 3: TEM micrograph of 5 phr sample at 40kX

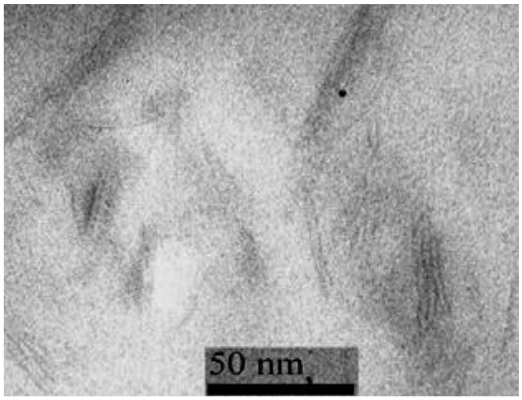

Figure 4: TEM micrograph of 3 phr sample at 40kX

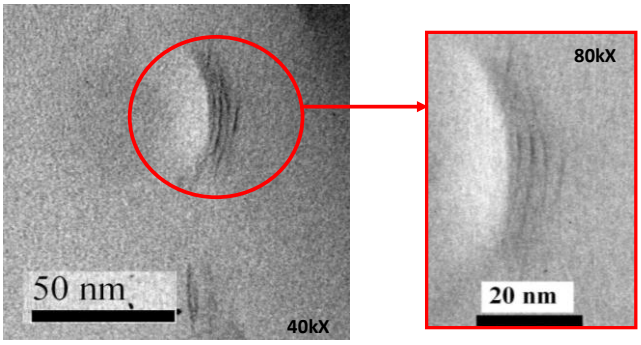

Figure 5: TEM micrograph of 1 phr sample at 40kX and 80kX magnification

The darker lines seen on the TEM images denote the layers of nanoclay, as it is composed of heavier elements such as Al, Si and O, whereas lighter atoms present in the polymer matrix are shown in brighter shade. The formation of intercalated nanocomposite is confirmed by these TEM micrographs, taken for 1, 3 and 5 phr content of nanoclay. The stack of silicate nanoclay measure at about 9-12 nm thick and visually, the interlayer distance is estimated to be between 3-4 nm, which is coherent with the XRD analysis. As for 7 phr sample, it exhibited no intercalation as the nanoclay agglomerates and form clots. Increasing nanoclay content from 5 phr onwards might make it difficult to disperse within polymer matrix.

Tensile Modulus and Tensile Strength

Figure 6 illustrates the tensile strength and the tensile modulus as a function of PMMA/N5 blend ratio.

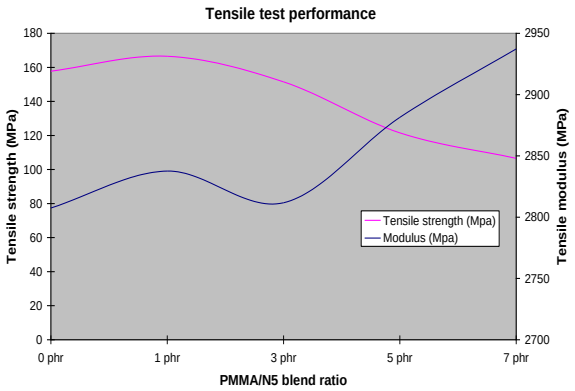

Figure 6: Characteristics of tensile performance

We can see clearly that there is an enhancement in both properties in 1 phr specimen compared to pure PMMA 0 phr specimen, which means that 1 phr reported here exhibits an improvement in elasticity, as well as in strength and modulus. This shows that there might be a good dispersion of nanoclay in the polymer matrix at this nanoclay loading. The tensile modulus substantially increases at higher content of nanoclay but at the same time the tensile strength gradually decreases from 1 phr onwards.

Several researchers, [11][12] have reported the weakening of the tensile strength in intercalated nanocomposites in function of the increasing nanoclay. This finding is attributed to the agglomeration of nanoparticles in the nanocomposite and/or the occurrence of influential sized voids in the microstructure. Both causes prevent the effective reinforcement of intercalated microstructure.

Hardness and Impact Test.

Characteristics on hardness and impact tests both exhibit similar trend, as seen in Figure 7; they decrease with an increasing of nanoclay content. This indicates that addition of nanoclay in the PMMA polymer did not enhance hardness and impact properties of the nanocomposite. The drop in impact strength observed along the increment of nanoclay content can be associated with the increase in brittleness of the material.

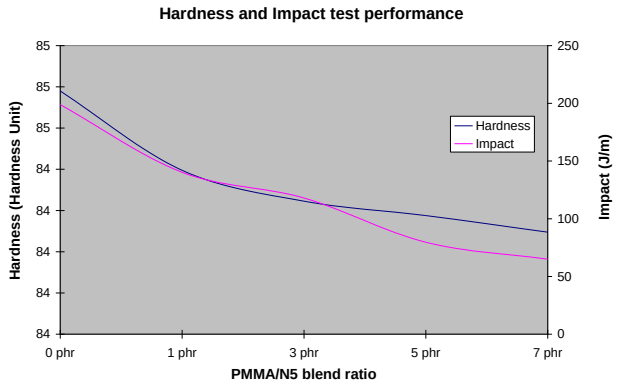

Figure 7: Characteristics of hardness and impact performance

Flexural Test

The reinforcement benefit of flexural strength notably in 1 phr specimen is indicated by the plot in Figure 8 of flexural strength at ultimate versus PMMA/nanoclay blend ratio. A significant 20% improvement of flexural strength is observed at 1 phr of nanoclay loading compared to pure PMMA, which indicates that it bends and resists deformation better under load. However, this strength drops off as the nanoclay loading increases, probably due to the presence of clustered clay nanoparticles. The clot possibly concentrated stress locally, leading to a decrease in the flexural performance of the nanocomposite [13][14].

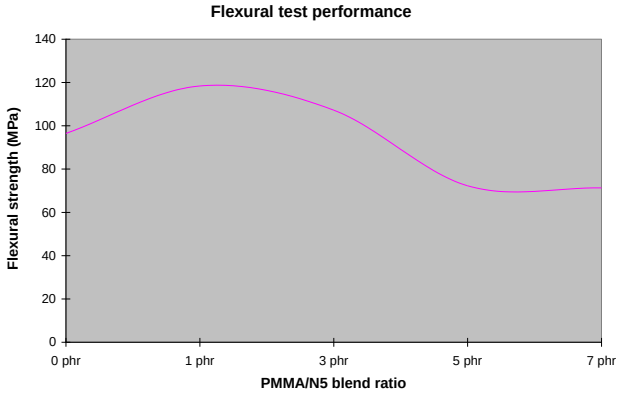

Figure 8: Characteristics of flexural performance

Specific Gravity.

The density value of each sample is shown in the following Figure 9.

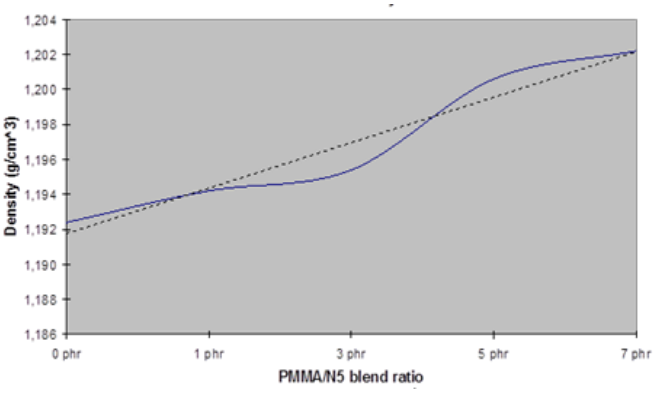

Figure 9: Specific Gravity of PMMA/Nanoclay

The density of pure PMMA (0 phr) is measured at 1,1924 g/cm^3. The density increases linearly with the increasing N5 loading in PMMA polymer matrix, which is anticipated, as the nanoclay is dispersed and inserted into the space volume available amongst the PMMA molecules.

Haze and Total Transmission Test.

Figure 10 shows the evolution of total transmittance and haze results measured by the hazemeter versus the PMMA/nanoclay blend ratio.

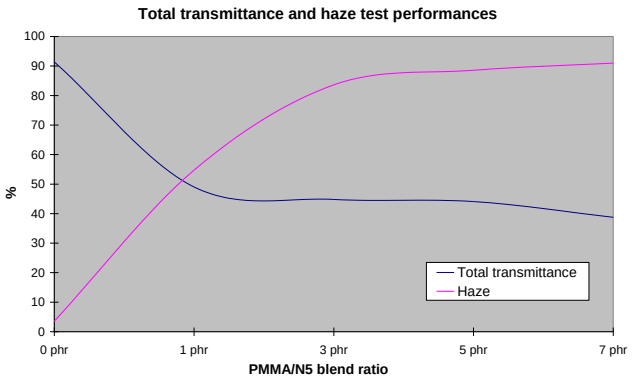

Figure 10: Characteristics of total transmittance and haze test

As the nanoclay content increases, the total transmittance decreases, rapidly from 0 phr to 1 phr until it reaches stability from 3 phr to 7 phr. This plot of total transmittance conforms to visual observation of the samples. The sample at 0 phr allows a visible light transmission of 91.42%, which is in good agreement with the literature - a total transmittance value of a pure PMMA is 92%. This proves that the sample is well-processed and moulded, producing a homogeneous material with a smooth surface. Some of the light will be reflected from the border surfaces and some will pass through the specimen unaltered, which will give glossy and see-through appearance for 0 phr. For other samples, the intensity of the transmitted light is diminished by the inherent absorbance of the materials.

On the other hand, the haze characteristic increases with the increasing nanoclay blend ratio. This is due to the increasing number of clay nanoparticles and irregularities in the material as seen in TEM micrographs. They act as scatterers of the incident light; the light is diffused uniformly in all directions, causing the light intensity per unit angle small. This diffuse scattering effect reduces contrast, resulting haze to increase.

Gloss Test.

The glossmeter gives out three values of gloss measured according to three standard incident angles of 20°,60° and 85°. According to the ASTM method D523, the 60° geometry is used as a reference, for comparing surfaces and to determine whether the 20° or 85° geometry is warranted. The following Figure 11 shows the characteristic of gloss at 20°,60° and 85° geometry.

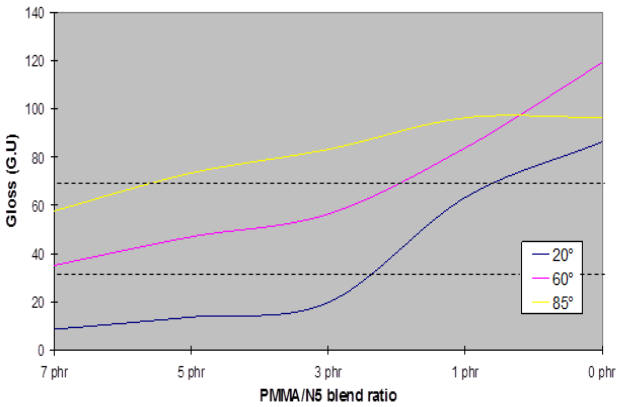

Figure 11: Characteristics of gloss test according to standard geometries 20˚,60˚ and 85˚

The 20° geometry is used when the sample has a value greater than 70 G.U for 60° gloss. It is classified as high gloss material, whereas the 85° is used if the value for 60° gloss is less than 30 G.U, where the material is classified as low gloss material. Therefore, the 0 and 1 phr samples are classified as high gloss materials, measured using 20° geometry, as they both has a value of 60° gloss greater than 70 G.U. The other samples; 3,5 and 7 phr on the other hand are considered as semi-gloss materials and measured using 60° geometry because their 60° gloss each value not less than 30 G.U.

Below is the new plot of latest gloss measurement, according to ASTM D523. A linear decreasing evolution can be seen from the Figure 12.

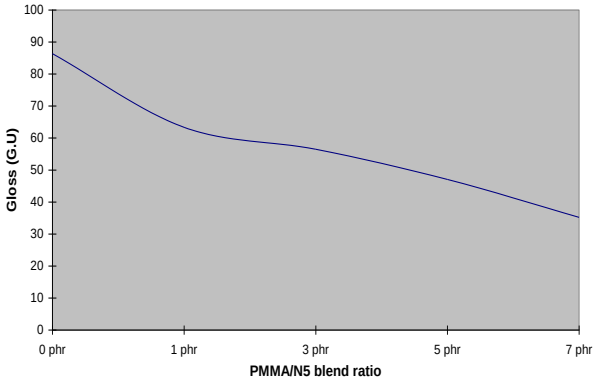

Figure 12: Characteristics of gloss test according to standard ASTM

The 0 and 1 phr sample are considered as high-gloss material, due to their smooth and polished surface which reflects the incident light directly on the surface in the main direction of reflection, where the angle of incidence is equal to the angle of reflection.

The 3, 5 and 7 phr sample are semi-gloss material, where the surface is rougher, leading the light to diffusely scattered in all directions. The more uniform the light is scattered, the less

intense the reflection in the main direction and the duller the surface will appear.

Abrasion Test.

Figure 13 illustrates the evolution of the haze and the weight loss before and after Taber abrasion test.

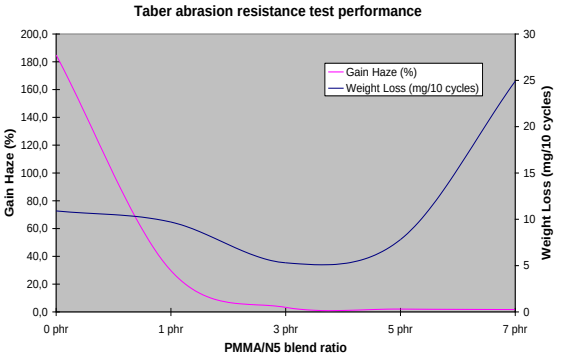

Figure 13: Evolution of the haze and the weight loss after Taber abrasion test.

Pure PMMA sample suffered the most variation of haze, which is reported nearly double of its original haze value. This also means that, although pure PMMA is the most transparent sample of all, upon any mechanical action, it would diffract the highest percentage of light, thus reducing the visual efficiency. However, it has a better abrasion resistance than 7 phr sample in term of weight loss.

The most optimum evolution goes for 3 phr sample, gaining only 3% haze and lost the minimal weight upon abrasion. Therefore, we can say that 3 phr sample is the sample which resisted the most against abrasion.

From the graph, we can generally summarize that, the more clay content there is, the lower the abrasion will cause in gaining haze but at the same time, the more it will lose in weight.

CONCLUSION

The development of the nanoclay/PMMA composites was successfully done via melt intercalation method in this research study. The effect of nanoclay particles within PMMA matrix was investigated. XRD analysis suggested the intercalation for 1, 3 and 5 phr nanocomposite specimens. Morphological characterization via TEM imaging confirmed the previous finding, while 7 phr nanocomposite exhibited agglomeration, suggesting bad dispersion within PMMA matrix. The stiffness of nanocomposite at higher filler loading increased, but its tensile strength decreased with higher nanoclay content. Increasing nanoclay content might induce higher brittleness in the nanocomposite. 1 phr nanocomposite appeared to be the most mechanically-enhanced specimen, as its tensile strength, tensile modulus and flexural increased in comparison to original PMMA (at 0 phr). On the other hand, the haze characteristic increases with the increasing nanoclay blend ratio. Furthermore, 3 phr sample is the sample which resisted the most against abrasion.

ACKNOWLEDGEMENT

The authors thank Dr Jamaliah Sharif and all personnel of Radiation Processing Division, Malaysia Nuclear Agency for technical assistance and guide during the research.

REFERENCES

[1] Dubois, A. 2000, “Polymer-Layered Silicate Nanocomposites : Preparation , Properties and Uses of a New Class of Material”, *Materials Science and Engineering*: R: Reports 28, no. 1 (2000): 1-63.

[2] Zanetti, M., Lomakin, S., and Camino, G. 2000, "Polymer layered silicate nanocomposites", *Macromolecular Materials and Engineering*, 279 (2000), p.p. 1-9.

[3] Okada, A., Kawasumi, M., Usuki, A., Kojima, Y., Kurauchi, T., and Kamigaito, O. 1990, “Synthesis and properties of nylon-6/clay hybrids”, In: Schaefer DW, Mark JE, editors. *Polymer based molecular composites*. MRS Symposium Proceedings, Pittsburgh, vol. 171; 1990. p. 45–50.

[4] Pavlidou, S., and Papaspyrides, C.D. 2008, “A review on polymer-layered silicate nanocomposites”, *Progress in Polymer Science 33* (2008); 1119-1198.

[5] LeBaron, P.C., Wang, Z., and Pinnavaia, T.J. 1999, “ Polymer–layered silicate nanocomposites: an overview”, *Appl Clay Sci* 1999;15:11–29.

[6] Hay, J. N. and S.J. Shaw. 2000, “Nanocomposites – Properties and Applications”, *A Review of Nanocomposites* 2000.

[7] Olad, A. 2011. Polymer/Clay Nanocomposites. *Advances in Diverse Industrial Applications of Nanocomposites*, Dr. Boreddy Reddy (Ed.), ISBN: 978-953-307-202-9, InTech

[8] Lokensgard, E. 2010. *Industrial Plastics: Theory and Applications*. Delmar, Cengage Learning, Clifton Park USA, fifth edition; 2010. p. 123-124

[9] Ray, S. and Okamoto, M. 2003, “New Polylactide/Layered Silicate Nanocomposites”, 6. *Macromol. Mater. Eng.*, 288: 936–944. doi: 10.1002/mame.20030015.

[10] Albdiry, M.T., and Yousif, B.F. 2013, “Fracture toughness and toughening mechanisms of unsaturated polyester-based clay nanocomposites,”

InICF13. 2013.

[11] Yasmin, A. 2003, "Processing of clay/epoxy nanocomposites by shear mixing", *Scripta Materialia*, Volume 49, Issue 1, Pages 81-86

[12] Peeterbroeck,S. 2004, "Polymer-Layered Silicate-Carbon Nanotube Nanocomposite: Unique Nanofiller Synergistic Effect", *Compos. Sci, Tecnolo*. 64, 2317-2323.

[13] Chow,W.S., Ishak, Z.A.M., Ishiaku, U.S., Karger-Kocsis, J., Apostolov, A.A. 2004, "The effect of organoclay on the mechanical properties and morphology of injection-molded polyamide polypropylene nanocomposites", *Journal of Applied Polymer Science*, vol. 91, no. 1, pp. 175–189.

[14] Mohanty, S., and Nayak, S.K. 2007, "Effect of clay exfoliation and organic modification on morphological, dynamic mechanical, and thermal behavior of melt-compounded polyamide-6 nanocomposites", *Polymer Composites*, vol. 28, no. 2, pp. 153–162.